Journal of Applied Physics ARTICLE scitation.org/journal/jap

Quantifying a partial polyamorphic transition in a cerium-based metallic glass during cooling

HPSTAR 1322-2021

Cite as: J. Appl. Phys. **130**, 145901 (2021); doi: 10.1063/5.0054997
Submitted: 24 April 2021 · Accepted: 24 September 2021 ·
Published Online: 12 October 2021

View Online Export Citation CrossMark

Zhi Chen,[1,2] Zhaoyue Sun,[1,2] Fujun Lan,[2] Xin Zhang,[2] Ziliang Yin,[2] Ye Liu,[2] Zhidan Zeng,[2] Yang Ren,[3] Hongbo Lou,[2,a)] Baolong Shen,[1] and Qiaoshi Zeng[1,2,a)]

AFFILIATIONS

[1]Jiangsu Key Laboratory of Advanced Metallic Materials, School of Materials Science and Engineering, Southeast University, Nanjing 211189, People's Republic of China
[2]Center for High Pressure Science and Technology Advanced Research, Pudong, Shanghai 201203, People's Republic of China
[3]X-ray Science Division, Argonne National Laboratory, Argonne, Illinois 60439, USA

[a)]**Authors to whom correspondence should be addressed:** hongbo.lou@hpstar.ac.cn and zengqs@hpstar.ac.cn

ABSTRACT

Cerium-based metallic glasses are prototype polyamorphous systems with pressure-induced polyamorphic transitions extensively reported. Cooling typically has a similar effect on materials as compression with regard to reducing volume. However, previous studies show dramatically different behavior of Ce-based metallic glasses between cooling and compression, whose origin remains unclear. Here, using *in situ* low-temperature synchrotron high-energy x-ray diffraction, the structural evolution of a $Ce_{68}Al_{10}Cu_{20}Co_2$ metallic glass is accurately determined and analyzed by a structure factor and a reduced pair distribution function (PDF) during cooling from 298 to 83 K. An unusually large linear thermal expansion coefficient is revealed, which is associated with both continuous but inconsistent structural changes between the two subpeaks of the first atomic shell in terms of average bond lengths and coordination numbers. These phenomena are suggested to be attributed to a gradual 4*f* electron delocalization of only a minimal amount (~2.6% at 83 K) of Ce atoms by quantitative analysis of the PDF data. However, a previously expected global polymorphic transition from a low-density amorphous state to a high-density amorphous state with an abrupt volume collapse is not observed. Moreover, electrical resistivity also shows a continuous increase during cooling without any sharp change. It is clarified that cryogenic temperatures could facilitate but are not powerful enough alone to trigger a global polymorphic transition in the $Ce_{68}Al_{10}Cu_{20}Co_2$ metallic glass, suggesting a wide distribution of its local atomic environment.

INTRODUCTION

It is common for crystalline materials to have chemically identical but structurally distinct phases, a phenomenon called polymorphism. Diamond and graphite are well-known examples of carbon polymorphism. However, glasses, at the extreme end of structural disordering, are usually thought to be structurally indistinguishable without identifiable structural symmetry. Surprisingly, with density change, Δρ, as the relevant order parameter, different amorphous states linked by pressure-induced polyamorphic transitions[1,2] have also been discovered in many open network glass systems[3–13] and recently even in closely packed metallic glasses (MGs).[14–29] The discovery of polyamorphism suggests the richness of the glass configurational space with distinct states, which not only deepens our fundamental understanding of glasses but also could lead to the development of switchable glass materials with identical composition but dramatically different physical properties.[30]

Ce-based MGs are the first MG systems that show pressure-induced polyamorphism in glasses with already maximized coordination numbers (12–14) of random nearest neighbors.[31,32] Pressure-induced electronic delocalization transitions of their 4*f* electrons in Ce atoms account for the bond shortening and densification,[14–16] which provides a distinct mechanism from the coordination number increase dominated bond lengthening (e.g., the Si–O and Ge–O bonds)[6,7] and densification in polyamorphous network glasses. Interestingly, the pressure-induced polyamorphic transitions in silica glass[33–35] and Ce-based MGs[18,36,37] share a common elastic anomaly with sound velocities (both compressional and shear waves) and bulk modulus minima during compression,

suggesting the elastic anomaly as a possible signature for polyamorphism.[36] Yu *et al.*[38] measured the temperature-dependent sound velocities (longitudinal: v_l, transverse: v_s) of $Ce_{68}Al_{10}Cu_{20}Co_2$ and $La_{68}Al_{10}Cu_{20}Co_2$ MGs from room temperature down to the liquid nitrogen temperature (77 K) using a pulse-echo overlap ultrasonic technique. Unlike the $La_{68}Al_{10}Cu_{20}Co_2$ MG with a normal stiffening behavior, the $Ce_{68}Al_{10}Cu_{20}Co_2$ MG exhibits an anomalous softening longitudinal sound mode and bulk modulus during cooling (decrease of the sound velocity, v_l, and bulk modulus), which is attributed to the mutable electronic structure and a possible electronic transition of 4*f* electrons in Ce. Counterintuitively, its transverse sound velocity still increases with decreasing temperature,[38] which differs from the consistent softening of both sound modes under compression.[36,37] Recent low-temperature synchrotron XRD studies on a $Ce_{62}Al_{10}Cu_{20}Co_8$ MG also revealed no sharp volume collapse, although a rather weak signal of 4*f* electron delocalization transition was observed by x-ray absorption spectroscopy (XAS) during cooling from 300 to 10 K.[39] Moreover, the linear length change from 300 to 77 K of $Ce_{68}Al_{10}Cu_{20}Co_2$ MG was determined to be ~0.34%,[38] which is much more pronounced than the $La_{68}Al_{10}Cu_{20}Co_2$ MG (~0.19%) and Zr/Cu-based MGs (~0.17%) during cooling at the same conditions.[38,39] In contrast, our previous work has shown that delocalization of 4*f* electrons in the $Ce_{68}Al_{10}Cu_{20}Co_2$ MG will cause a polyamorphic transition from a low-density amorphous state to a high-density amorphous state with a density increase of ~9.6%;[40] thus, a linear length change of ~3.2%, which is one order of magnitude larger than the temperature-induced shrinkage, makes a similar polymorphic transition during cooling unlikely.

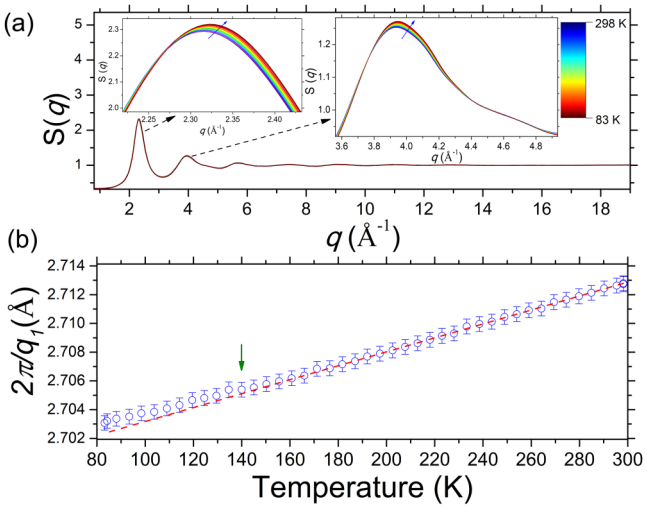

FIG. 1. Structural evolution of the $Ce_{68}Al_{10}Cu_{20}Co_2$ MG upon cooling from 298 to 83 K in reciprocal space. (a) Structure factor, S(*q*), of the $Ce_{68}Al_{10}Cu_{20}Co_2$ MG. The two insets are the zoomed plots for the first (2.22–2.43 Å^{-1}) and second (3.55–4.93 Å^{-1}) peaks in S(*q*) as marked by the black dashed arrows, respectively. The blue arrows in the insets point to the directions of peak changes during cooling. (b) Inverse peak position, $2\pi/q_1$, obtained by fitting the first peak of S(*q*) using a Voigt function (blue open circles). The dashed red line is the linear fit of the relatively high-temperature part (>200 K) of the $2\pi/q_1$ data. The green arrow denotes the temperature where the $2\pi/q_1$ data positively deviate from the linear fit.

On the other hand, it has been observed that both cooling and compression could induce the delocalization of 4*f* electrons accounting for the polymorphic γ-to-α transitions in pure Ce and Ce-bearing crystalline alloys.[41–43] One may expect that the low-temperature elastic anomalies in Ce-based MGs may be related to the delocalization of the 4*f* electrons as well. However, a careful comparison between cooling and compression induced structural changes in Ce-based MG systems has never been reported. Assuming the irregular larger contraction (excess amount of volume contraction compared with the $La_{68}Al_{10}Cu_{20}Co_2$ MG) during cooling is indeed due to the 4*f* electron delocalization in the $Ce_{68}Al_{10}Cu_{20}Co_2$ MG,[38] and all the 4*f* electrons become delocalized in the previous high-pressure experiments;[40] the percentage of the Ce atoms in the $Ce_{68}Al_{10}Cu_{20}Co_2$ MG participated in the 4*f* electron delocalization transition from room temperature to 77 K can be estimated to be only (0.34%–0.19%)/3.2% ≈ 4.7%. It is pretty surprising, and so far, no experimental evidence to support this speculation, which hinders our comprehensive understanding of the polyamorphism in MGs in the pressure-temperature two-dimensional space and the effect of structural disorder on 4*f* electron systems.

In this work, the prototype $Ce_{68}Al_{10}Cu_{20}Co_2$ MG is chosen as an extensively studied system with a lot of unusual low-temperature[38] and high-pressure[36,40] behavior reported. By using *in situ* low-temperature synchrotron high-energy x-ray diffraction (XRD), the structure factor, *S*(*q*), and reduced pair distribution function, *G*(*r*), are obtained as a function of temperature from 298 down to 83 K. The sample's thermal expansion coefficient and detailed structural changes in both reciprocal space and real space are derived and quantitatively analyzed, whose correlation with possible temperature-induced polyamorphic transition is discussed and clarified. By comparing the high-pressure and low-temperature behavior, we found that the amount of Ce atoms participated in the 4*f* electron delocalization can be quantitatively estimated from the information of structural changes in real space (bond shortening and coordination number changes in sub-shells), which could help to better understand the various anomalous behavior of *f*-electron bearing MGs with changing temperature or pressure.

EXPERIMENTAL

Master ingots with a nominal composition of $Ce_{68}Al_{10}Cu_{20}Co_2$ were prepared by arc-melting a mixture of commercial-purity Ce (99.5 wt.%) with high-purity Al (99.99 at.%), Cu (99.99 at.%), and Co (99.99 at.%) in a zirconium-gettered high-purity argon atmosphere. Ingots were all re-melted five times to ensure their chemical homogeneity. $Ce_{68}Al_{10}Cu_{20}Co_2$ MG rod samples were prepared by copper-mold casting the master ingots into cylinders with a diameter of ~2 mm. $Ce_{68}Al_{10}Cu_{20}Co_2$ MG ribbon samples with a thickness of ~30 μm and a width of ~2 mm were prepared from the master ingots using a single roller melt-spinning system. The glass nature of the prepared samples was verified by XRD and differential scanning calorimetry (DSC), which are consistent with previous reports.[38,44]

A disk with a thickness of ~500 um was cut from the cylinder samples for *in situ* low-temperature synchrotron high-energy XRD at the beamline 11-ID-C of Advanced Photon Source (APS), Argonne National Laboratory (ANL), USA. The x-ray wavelength was 0.111 65 Å, and the x-ray beam size was set to be $0.5 \times 0.5\ mm^2$ defined by slits. The $Ce_{68}Al_{10}Cu_{20}Co_2$ MG sample was cooled at 10 K/min in a Linkam THMS600 stage with the temperature accuracy of 0.01 K. The exposure time for each diffraction pattern was set to 30 s with a temperature resolution of around 5 K per pattern. Two-dimensional (2D) XRD images were collected continuously during cooling by a PerkinElmer amorphous silicon detector, with a maximum wavevector momentum transfer of $q = 19\ Å^{-1}$. Then, the 2D images were integrated into one-dimensional $I(q)$ data with the software Dioptas. $S(q)$ and $G(r)$ data were further derived using the program package PDFgetX3.[17]

The standard four-probe method was employed for a low-temperature electrical resistance measurement of the $Ce_{68}Al_{10}Cu_{20}Co_2$ MG ribbon samples. A constant current of 20 mA was supplied by a current source (Keithley-6221), and the voltage of the sample was measured by a nano-voltmeter (Keithley-2182A). The low-temperature environment was controlled by a Linkam HFS600E-PB4 probe stage with a temperature accuracy of 0.01 K.

RESULTS AND DISCUSSION

Figure 1(a) shows the $S(q)$ of $Ce_{68}Al_{10}Cu_{20}Co_2$ MG upon cooling from 298 to 83 K. The $S(q)$ patterns present typical amorphous features with a limited number of broad peaks, and the peak intensity quickly decays with increasing q. There are no obvious changes caused by structural transitions or crystallizations over the entire temperature range, as shown in Fig. 1(a). All the patterns seem to coincide with each other, and the temperature-induced changes are subtle as expected, which is consistent with the previous report in other MGs.[45] The insets of Fig. 1(a) present the enlarged plots of the first (2.22–2.43 $Å^{-1}$) and second (3.55–4.93 $Å^{-1}$) peaks of $S(q)$. A consistent increase of peak intensity and right-shifting peak positions with cooling can be observed, mainly attributed to cooling-induced structural shrinkage,[46] which resembles the pressure-induced structural densification in the $Ce_{68}Al_{10}Cu_{20}Co_2$ MG but within a much smaller amplitude.[40] It should be noted that high-pressure causes splitting of the second peak, and a much stronger subpeak emerges at the right shoulder of the second peak, which is one of the most significant features in $S(q)$ associated with the polyamorphic transition.[14,25] In contrast, the right shoulder of the second peak of $S(q)$ remains almost constant during cooling, which seems against the previous speculation of a temperature-induced polyamorphic transition[38,39] and suggests that cooling-induced structural changes have their own feature different from compression of the Ce-based MGs.

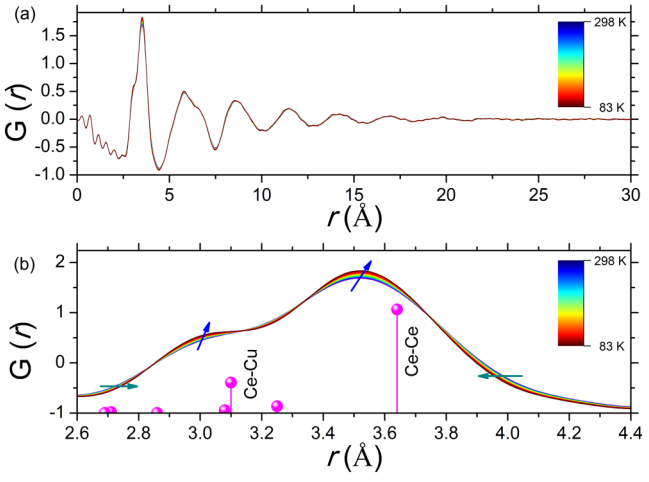

FIG. 2. Structural evolution of the $Ce_{68}Al_{10}Cu_{20}Co_2$ MG upon cooling from 298 to 83 K in real space. (a) Reduced pair distribution function, $G(r)$, of the $Ce_{68}Al_{10}Cu_{20}Co_2$ MG. (b) The zoomed plot of the first peak in $G(r)$. The arrows point to the directions of peak changes during cooling. The ball symbols with drop lines represent the bond distances in the first atomic shell based on a hard-sphere model.[51] The height of the drop lines corresponds to the weight value of each atomic pair.

Figure 1(b) shows the inverse peak position of the first peak of $S(q)$, $2\pi/q_1$, as a function of temperature. According to the previous work, $2\pi/q_1$ is proportional to the average atomic spacing in MGs and could give a perfect estimation of the linear thermal expansion with varying temperatures.[45] The data in Fig. 1(b) show a linear behavior above ~140 K with a linear expansion coefficient of $(4.85 \pm 0.03) \times 10^{-5}\ K^{-1}$. This value is much larger (~3 times) than the typical values of other regular MGs measured by similar XRD techniques, e.g., $\sim 1.66 \times 10^{-5}\ K^{-1}$ for the $Pd_{40}Cu_{30}Ni_{10}P_{20}$ MG,[45] $\sim 1.4 \times 10^{-5}\ K^{-1}$ for the $La_{62}Al_{14}(Cu_{5/6}Ag_{1/6})_{14}Ni_5Co_5$ MG,[47] and $\sim 1.1 \times 10^{-5}\ K^{-1}$ for the $Zr_{60}Ti_2Cu_{20}Ni_8Al_{10}$ MG[48] but supports the observation of an anomalous large length change of the $Ce_{68}Al_{10}Cu_{20}Co_2$ MG compared with the other La-based and Zr/Cu-based MGs cooling from room temperature to the liquid nitrogen temperature.[38,39] When the temperature is below ~140 K, the decrease of $2\pi/q_1$ slows down and starts to deviate from the initial linear trend.

After Fourier transformation, $G(r)$ can be derived from $S(q)$, which offers structural information in real space in terms of a probability distribution of interatomic pair correlations as shown in Fig. 2(a). The quickly vanished oscillations above ~20 Å confirm a highly disordered glass structure of the MG sample. Similar to the $S(q)$ patterns, all the $G(r)$ patterns almost coincide with each other during cooling. Since a typical pressure-induced polyamorphic transition usually causes abrupt bond shortening, the first peak of $G(r)$ is zoomed in Fig. 2(b) for more careful analysis. The first peak of $G(r)$ mainly consists of two subpeaks, which show a consistent increase of peak intensities, narrowing of peak widths, and right-shifting of positions during cooling. Although the changes of peak intensities and widths are consistent with the consequence of a temperature decrease based on the framework of the Debye theory,[48] the right-shifting of both peak positions seems counter-intuitive because it means that the bonds expand rather than bonds contract during cooling. The previous work on melts of pure metals has observed similar phenomena attributed to the inverse proportional relationship between coordination numbers in the first atomic shell and temperatures,[46,49] as well as in many multi-

component MG systems.[46] Therefore, it seems that no unusual phenomenon is directly associated with a possible cooling-induced polyamorphic transition.

Although in total, there are ten different atomic pairs in a four-component alloy such as the $Ce_{68}Al_{10}Cu_{20}Co_2$ MG, due to the significant differences in x-ray scattering factors and concentrations between the four components, only two atomic pairs have the dominant contributions to the first peak of $G(r)$ with two of the highest weights, w_{ij}, i.e., the Ce–Ce (w_{ij}: 0.701 72) and Ce–Cu (w_{ij}: 0.206 43) atomic pairs as denoted in Fig. 2(b). Therefore, it is reasonable to have two Gaussian peaks to fit the first peak of $G(r)$, which was an extensively employed method for quantitative analysis of $G(r)$ in MGs.[50,51] The fitting results of normalized subpeak positions ($r/r_{298\ K}$), widths ($W/W_{298\ K}$), areas ($A/A_{298\ K}$), and area changes over the total peak area ($\Delta A_{sub}/A_{total}$) are shown in Fig. 3. The width changes are pretty consistent between the two subpeaks. In contrast, the peak position and the area of the first subpeak (Ce–Cu pair dominated, denoted as subpeak-11 in the figure) change much more dramatically than the second subpeak (Ce–Ce pair dominated, denoted as subpeak-12 in the figure). Notably, the area of the first subpeak increases, while that of the second subpeak slightly decreases upon cooling. Since the peak area in $G(r)$ is proportional to its corresponding coordination number, it is likely that some neighbor atoms in the second subpeak gradually move into the first subpeak with shorter bond lengths. This speculation is in line with changes in the pressure-induced polyamorphic transitions in Ce-bearing MGs.[14,16] Specifically, pressure-induced delocalization of 4*f* electrons in Ce causes the Ce–Ce bond length shortening and Ce atomic volume collapse. Therefore, the first peak of the partial $G(r)$ of Ce–Ce pairs will split, and a new subpeak emerges with a much shorter bond length at the expense of the initial Ce–Ce subpeak intensity.[14] Actually, temperature-induced γ-to-α transitions at constant pressures in pure crystalline Ce and Ce-bearing alloys have been extensively observed. Lower pressure is usually required to trigger their transitions with decreasing temperature.[41–43] Therefore, it is reasonable to attribute the abnormal area decrease of the second subpeak in the first $G(r)$ peak of the $Ce_{68}Al_{10}Cu_{20}Co_2$ MG to the temperature-induced 4*f* electron delocalization at ambient pressure. This speculation also could rationalize the much smaller linear coefficient of the second subpeak shift upon cooling [Fig. 3(a)]; i.e., cooling-induced coordination number increase is partially compensated for by the 4*f* delocalization of Ce atoms. However, it should be noted that due to the diverse environment (intrinsic structural heterogeneity) of the Ce atoms in a glass structure, the critical temperature or pressure for the 4*f* delocalization of each individual Ce atom could have a wide distribution. Therefore, only a tiny portion of Ce atoms may gradually satisfy the criterion to show 4*f* delocalization transitions by decreasing temperature, which does not cause a sharp global volume collapse, and, therefore, is manifested as continuous changes in $S(q)$ and the linear thermal expansion coefficient measurement. According to the relative subpeak area change over the almost constant area of the whole first peak of $G(r)$ as shown in Fig. 3(d), $\Delta A_{11}/(A_{11}+A_{12})$ or $\Delta A_{12}/(A_{11}+A_{12})$, a rough estimation of the portion of Ce atoms that participate in the possible 4*f* delocalization is as small as $\sim(2.6 \pm 0.6)\%$ down to 83 K. This small

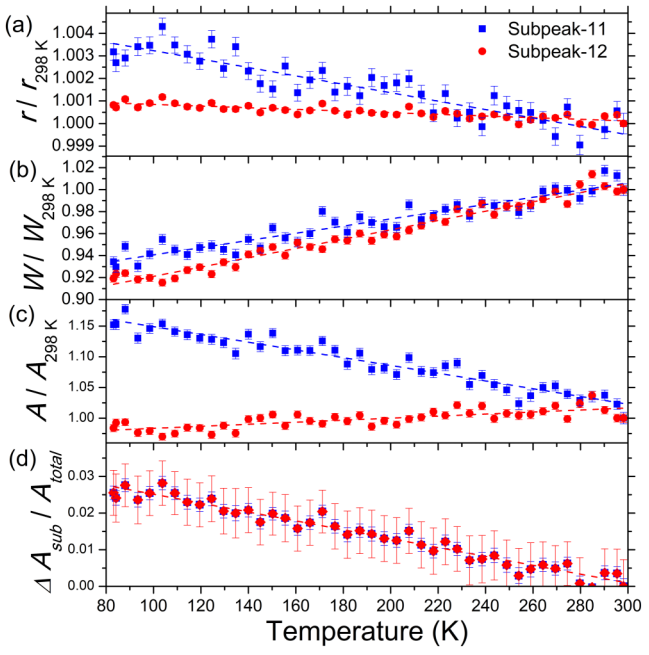

FIG. 3. Relative changes of the fitted Gaussian profile parameters of the two subpeaks in the first peak of $G(r)$ from 298 to 83 K. (a) Peak position *r*. (b) Peak width *W*. (c) Subpeak area *A*. (d) Change of the subpeak area over a total peak area, $(A_{11} - A_{11\_298\ K})/A$ and $(A_{12\_298\ K} - A_{12})/A$. The two data sets overlap with each other very well because the area of the whole first peak of $G(r)$ remains almost constant during cooling. The dashed lines are linear fits of the data. Subpeak-11 (blue squares) and subpeak-12 (red circle) represent the Ce–Cu and Ce–Ce dominated atomic pairs, respectively.

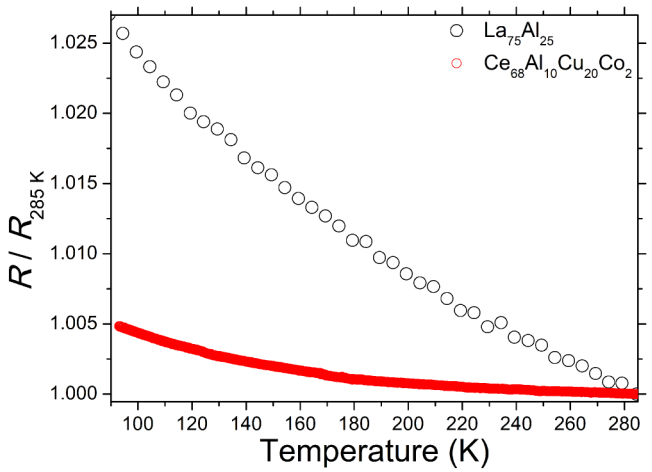

FIG. 4. Relative changes of resistivity ($R/R_{285\ K}$) of the $Ce_{68}Al_{10}Cu_{20}Co_2$ MG from 285 to 93 K (red circles) compared with data of the $La_{75}Al_{25}$ MG from Ref. 53 (black circles).

value reasonably matches the value estimated from the linear length change (~4.7% at 77 K), which suggests that the high-pressure and the low-temperature do have a similar effect on the 4*f* electron behavior in the MG system. This also explains the anomalous large thermal expansion coefficient estimated from the thermal shift of the principal peak of $S(q)$ but without an abrupt change due to the continuous 4*f* electron delocalization of only a small portion of the Ce atoms. The slope deviation at around 140 K in the $2\pi/q_1$ vs T in Fig. 1(b) is still unclear. More experiments are needed to address if this positive deviation is due to the slowing down of the 4*f*-electron delocalization. Thus, other than sophisticated XAS experiment detecting the electron state change in Ce-based MGs,[16,20,39] we show that atomic structural changes in both reciprocal ($S(q)$) and real space ($G(r)$) could be employed as an alternative ready method to monitor the delocalization of 4*f* electrons associated with Ce–Ce bond shortening.

Electrical resistivity of MGs is also a sensitive structural probe, which usually shows pronounced drops through the pressure-induced polyamorphic transitions during compression.[17,52,53] The electrical resistivity measurement of the $Ce_{68}Al_{10}Cu_{20}Co_2$ MG during cooling (Fig. 4) shows a very similar trend with the alloy without 4*f* electrons, the $La_{75}Al_{25}$ MG,[54] confirming the continuous evolution of the structure as well. Nevertheless, it should be noted that the temperature coefficient of resistivity (TCR) of the $Ce_{68}Al_{10}Cu_{20}Co_2$ MG is much smaller (~one fifth at 93 K) than that of the $La_{75}Al_{25}$ MG, which could be associated with the gradually increased number of conduction electrons due to the continuous 4*f* electron delocalization during cooling. However, a transition from negative to positive TCR reported in Ce-based MG under high pressure[17] has not been achieved yet by cooling, which further indicates that cooling along at ambient pressure is not as powerful as pressure in intriguing global polyamorphic transitions in Ce-based MGs.

SUMMARY

In conclusion, by monitoring the structural evolution of a prototype polyamorphous $Ce_{68}Al_{10}Cu_{20}Co_2$ MG using the *in situ* low-temperature high-energy synchrotron XRD, detailed structural information in both reciprocal space [$S(q)$] and real space [$G(r)$] are obtained as a function of temperature from 298 down to 83 K. Although there are no abrupt changes in the $S(q)$ indicating the absence of a global temperature-induced polyamorphic transition, the unusually large linear thermal expansion coefficient estimated from the thermal shift of the principal peak of $S(q)$ can be attributed to the continuous delocalization of 4*f* electrons in a small portion of Ce atoms. Moreover, quantitative analysis of the two subpeaks of the first peak of $G(r)$ shows inconsistent changes; i.e., the second subpeak mainly originated from the Ce–Ce atomic pairs shows a peak area decrease, which resembles the typical 4*f* electron delocalization transition observed previously in other Ce-bearing MGs under high pressures. The amount of Ce atoms that participated in the possible polyamorphic transition is minimal, ~(2.6 ± 0.6)% at 83 K, according to the relative subpeak area change over the total area of the first peak in $G(r)$, which matches reasonably well with the value estimated from linear thermal contraction (~4.7% at 77 K). The low-temperature electrical resistivity measurement confirms the continuous structural changes during cooling associated with 4*f* electron delocalization. These results provide a rational explanation for the previously reported anomalous phonon softening (decrease of the longitudinal sound velocity and bulk modulus) upon cooling[38] in the $Ce_{68}Al_{10}Cu_{20}Co_2$ MG and also clarify that temperature alone is not powerful enough to trigger a global polyamorphic transition associated with the 4*f* electron delocalization as reported under high pressure in the Ce-based MGs. The opposite trends of transverse sound modes observed during cooling (stiffening)[38] and compression (softening)[36,37] can be explained by the relatively low sensitivity of transverse sound velocity to external stimuli (e.g., much smaller dv/dP)[36,37] and limited tuning power of cooling compared to high pressure compression on the Ce-based MGs. These results also suggest that the local environment of Ce atoms in the glass structure is quite diverse with a wide distribution, and only a very small portion of the Ce atoms could gradually satisfy the conditions for the 4*f* electron delocalization during cooling at ambient pressure. On the other hand, it is demonstrated that Ce atoms with pressure or temperature-induced 4*f* electron delocalization could be employed as a sensitive probe for a local structural heterogeneity study of MGs in the future.

ACKNOWLEDGMENTS

This research was supported by the National Natural Science Foundation of China (NSFC) (Grant Nos. 51871054 and U1930401). The *in situ* low-temperature high-energy XRD experiment was performed at the beamline 11-ID-C, APS, ANL. The APS is a U.S. Department of Energy (DOE) Office of Science User Facility operated for the DOE Office of Science by ANL under Contract No. DE-AC02-06CH11357.

AUTHOR DECLARATIONS

Conflict of Interest

The authors have no conflicts to disclose.

Author Contributions

Z.C. and Z.S. contributed equally to this work.

DATA AVAILABILITY

The data that support the findings of this study are available from the corresponding authors upon reasonable request.

REFERENCES

[1]P. F. McMillan, J. Mater. Chem. **14**, 1506 (2004).
[2]D. Machon, F. Meersman, M. C. Wilding, M. Wilson, and P. F. McMillan, Prog. Mater. Sci. **61**, 216 (2014).
[3]O. Mishima and Y. Suzuki, Nature **419**, 599 (2002).
[4]C. A. Tulk, C. J. Benmore, J. Urquidi, D. D. Klug, J. Neuefeind, B. Tomberli, and P. Egelstaff, Science **297**, 1320 (2002).
[5]J.-P. Itié, A. Polian, G. Calas, J. Petiau, A. Fontaine, and H. Tolentino, Phys. Rev. Lett. **63**, 398 (1989).
[6]C. Meade, R. J. Hemley, and H. K. Mao, Phys. Rev. Lett. **69**, 1387 (1992).
[7]M. Guthrie, C. A. Tulk, C. J. Benmore, J. Xu, J. L. Yarger, D. D. Klug, J. S. Tse, H. K. Mao, and R. J. Hemley, Phys. Rev. Lett. **93**, 115502 (2004).

[8]S. K. Lee, P. J. Eng, H. K. Mao, Y. Meng, and J. Shu, Phys. Rev. Lett. **98**, 105502 (2007).
[9]E. Soignard, S. A. Amin, Q. Mei, C. J. Benmore, and J. L. Yarger, Phys. Rev. B **77**, 144113 (2008).
[10]P. F. McMillan, M. Wilson, D. Daisenberger, and D. Machon, Nat. Mater. **4**, 680 (2005).
[11]M. H. Bhat, V. Molinero, E. Soignard, V. C. Solomon, S. Sastry, J. L. Yarger, and C. A. Angell, Nature **448**, 787 (2007).
[12]W. A. Crichton, M. Mezouar, T. Grande, S. Stolen, and A. Grzechnik, Nature **414**, 622 (2001).
[13]Q. Mei, C. J. Benmore, R. T. Hart, E. Bychkov, P. S. Salmon, C. D. Martin, F. M. Michel, S. M. Antao, P. J. Chupas, P. L. Lee, S. D. Shastri, J. B. Parise, K. Leinenweber, S. Amin, and J. L. Yarger, Phys. Rev. B **74**, 014203 (2006).
[14]H. W. Sheng, H. Z. Liu, Y. Q. Cheng, J. Wen, P. L. Lee, W. K. Luo, S. D. Shastri, and E. Ma, Nat. Mater. **6**, 192 (2007).
[15]Q. S. Zeng, Y. C. Li, C. M. Feng, P. Liermann, M. Somayazulu, G. Y. Shen, H. K. Mao, R. Yang, J. Liu, T. D. Hu, and J. Z. Jiang, Proc. Natl. Acad. Sci. U.S.A. **104**, 13565 (2007).
[16]Q. S. Zeng, Y. Ding, W. L. Mao, W. G. Yang, S. V. Sinogeikin, J. F. Shu, H. K. Mao, and J. Z. Jiang, Phys. Rev. Lett. **104**, 105702 (2010).
[17]Q. S. Zeng, V. V. Struzhkin, Y. Z. Fang, C. X. Gao, H. B. Luo, X. D. Wang, C. Lathe, W. L. Mao, F. M. Wu, H. K. Mao, and J. Z. Jiang, Phys. Rev. B **82**, 054111 (2010).
[18]M. J. Duarte, P. Bruna, E. Pineda, D. Crespo, G. Garbarino, R. Verbeni, K. Zhao, W. H. Wang, A. H. Romero, and J. Serrano, Phys. Rev. B **84**, 224116 (2011).
[19]G. Li, Y. Y. Wang, P. K. Liaw, Y. C. Li, and R. P. Liu, Phys. Rev. Lett. **109**, 125501 (2012).
[20]L. Belhadi, F. Decremps, S. Pascarelli, L. Cormier, Y. Le Godec, S. Gorsse, F. Baudelet, C. Marini, and G. Garbarino, Appl. Phys. Lett. **103**, 111905 (2013).
[21]W. Zhao, Y. Y. Wang, R. P. Liu, and G. Li, Appl. Phys. Lett. **102**, 031903 (2013).
[22]C. L. Lin, A. S. Ahmad, H. B. Lou, X. D. Wang, Q. P. Cao, Y. C. Li, J. Liu, T. D. Hu, D. X. Zhang, and J. Z. Jiang, J. Appl. Phys. **114**, 213516 (2013).
[23]Y. Y. Wang, W. Zhao, G. Li, Y. C. Li, and R. P. Liu, Mater. Lett. **110**, 184 (2013).
[24]Q. Luo, G. Garbarino, B. Sun, D. Fan, Y. Zhang, Z. Wang, Y. Sun, J. Jiao, X. Li, P. Li, N. Mattern, J. Eckert, and J. Shen, Nat. Commun. **6**, 5703 (2015).
[25]F. Decremps, G. Morard, G. Garbarino, and M. Casula, Phys. Rev. B **93**, 054209 (2016).
[26]Z. Yin, H. Lou, H. Sheng, Z. Zeng, W. L. Mao, and Q. Zeng, J. Appl. Phys. **129**, 025108 (2021).
[27]Q. Du, X.-J. Liu, Q. Zeng, H. Fan, H. Wang, Y. Wu, S.-W. Chen, and Z.-P. Lu, Phys. Rev. B **99**, 014208 (2019).
[28]D. Singh, S. Basu, R. K. Mandal, O. N. Srivastava, and R. S. Tiwari, Intermetallics **67**, 87 (2015).
[29]H. B. Lou, Y. K. Fang, Q. S. Zeng, Y. H. Lu, X. D. Wang, Q. P. Cao, K. Yang, X. H. Yu, L. Zheng, Y. D. Zhao, W. S. Chu, T. D. Hu, Z. Y. Wu, R. Ahuja, and J. Z. Jiang, Sci. Rep. **2**, 376 (2012).
[30]P. H. Poole, T. Grande, C. A. Angell, and P. F. McMillan, Science **275**, 322 (1997).
[31]H. W. Sheng, W. K. Luo, F. M. Alamgir, J. M. Bai, and E. Ma, Nature **439**, 419 (2006).
[32]D. B. Miracle, Nat. Mater. **3**, 697 (2004).
[33]K. i. Kondo, S. Iio, and A. Sawaoka, J. Appl. Phys. **52**, 2826 (1981).
[34]C.-s. Zha, R. J. Hemley, H.-k. Mao, T. S. Duffy, and C. Meade, Phys. Rev. B **50**, 13105 (1994).
[35]Y. Kono, A. Yamada, Y. Wang, T. Yu, and T. Inoue, Rev. Sci. Instrum. **82**, 023906 (2011).
[36]Q. Zeng, Z. Zeng, H. Lou, Y. Kono, B. Zhang, C. Kenney-Benson, C. Park, and W. L. Mao, Appl. Phys. Lett. **110**, 221902 (2017).
[37]B. Zhang, R. J. Wang, and W. H. Wang, Phys. Rev. B **72**, 104205 (2005).
[38]P. Yu, R. J. Wang, D. Q. Zhao, and H. Y. Bai, Appl. Phys. Lett. **91**, 201911 (2007).
[39]Q. Luo, B. Schwarz, J. C. Swarbrick, J. Bednarčik, Y. Zhu, M. Tang, L. Zheng, R. Li, J. Shen, and J. Eckert, Phys. Rev. B **97**, 064104 (2018).
[40]Q. S. Zeng, Y. Lin, Y. J. Liu, Z. D. Zeng, C. Y. Shi, B. Zhang, H. B. Lou, S. V. Sinogeikin, Y. Kono, C. Kenney-Benson, C. Y. Park, W. G. Yang, W. H. Wang, H. W. Sheng, H. K. Mao, and W. L. Mao, Proc. Natl. Acad. Sci. U.S.A. **113**, 1714 (2016).
[41]J. D. Thompson, Z. Fisk, J. M. Lawrence, J. L. Smith, and R. M. Martin, Phys. Rev. Lett. **50**, 1081 (1983).
[42]J. M. Lawrence, P. S. Riseborough, and R. D. Parks, Rep. Prog. Phys. **44**, 1 (1981).
[43]M. J. Lipp, D. Jackson, H. Cynn, C. Aracne, W. J. Evans, and A. K. McMahan, Phys. Rev. Lett. **101**, 165703 (2008).
[44]X. F. Liu, R. J. Wang, D. Q. Zhao, M. X. Pan, and W. H. Wang, Appl. Phys. Lett. **91**, 041901 (2007).
[45]A. R. Yavari, A. L. Moulec, A. Inoue, N. Nishiyama, N. Lupu, E. Matsubara, W. J. Botta, G. Vaughan, M. D. Michiel, and Å Kvick, Acta Mater. **53**, 1611 (2005).
[46]X. Bian, G. Wang, Q. Wang, B. Sun, I. Hussain, Q. Zhai, N. Mattern, J. Bednarčík, and J. Eckert, Mater. Res. Lett. **5**, 284 (2017).
[47]J. Bednarcik, S. Michalik, M. Sikorski, C. Curfs, X. D. Wang, J. Z. Jiang, and H. Franz, J. Phys. Condens. Matter **23**, 254204 (2011).
[48]N. Mattern, U. Kühn, H. Hermann, S. Roth, H. Vinzelberg, and J. Eckert, Mater. Sci. Eng., A **375–377**, 351 (2004).
[49]H. Lou, X. Wang, Q. Cao, D. Zhang, J. Zhang, T. Hu, H.-k. Mao, and J.-Z. Jiang, Proc. Natl. Acad. Sci. U.S.A. **110**, 10068 (2013).
[50]K. Georgarakis, D. V. Louzguine-Luzgin, J. Antonowicz, G. Vaughan, A. R. Yavari, T. Egami, and A. Inoue, Acta Mater. **59**, 708 (2011).
[51]N. Mattern, U. Kühn, H. Hermann, H. Ehrenberg, J. Neuefeind, and J. Eckert, Acta Mater. **50**, 305 (2002).
[52]H. B. Lou, Z. D. Zeng, F. Zhang, S. Y. Chen, P. Luo, X. H. Chen, Y. Ren, V. B. Prakapenka, C. Prescher, X. B. Zuo, T. Li, G. Wen, W. H. Wang, H. S. Sheng, and Q. S. Zeng, Nat. Commun. **11**, 314 (2020).
[53]L. Zhang, J. Wang, F. Tang, H. Yang, X. Liu, Y. Zhao, and W. Yang, High Press. Res. **37**, 11 (2017).
[54]Q. Zeng, C. Rotundu, W. Mao, J. Dai, Y. Xiao, P. Chow, X.-J. Chen, C. Qin, H.-k. Mao, and J. Jiang, J. Appl. Phys. **109**, 113716 (2011).